Detecting Corrosion of Steel Prestressing Strands Using Acoustic Emission

Mohamed K. ElBatanouny[1], Jesé Mangual[1], Paul Ziehl[2], and Fabio Matta[3]

[1] *Graduate Research Assistant, University of South Carolina, Columbia, SC, 29208*
elbatano@email.sc.edu
mangualj@email.sc.edu

[2] *Associate professor, University of South Carolina, Columbia, SC, 29208*
ziehl@cec.sc.edu

[3] *Assistant professor, University of South Carolina, Columbia, SC, 29208*
mattaf@cec.sc.edu

ABSTRACT

America's transportation infrastructure has been receiving intensive public and private attention in recent years, particularly highway bridges. Corrosion of reinforcement steel is a main durability issue especially for concrete structures present in coastal areas and in areas where de-icing salts are routinely used.

Acoustic emission (AE) is a promising method for detecting corrosion in steel reinforced concrete members. This type of non-destructive testing (NDT) method primarily measures the magnitude of energy released within a material when physically strained. The expansive ferrous product resulting from corrosion induces pressure at the steel-concrete interface creating micro-cracks which can be detected by AE sensors. In this study, five concrete blocks with embedded prestressing steel strands were built and tested under accelerated corrosion conditions to evaluate possible correlations between AE activity and the onset and progression of corrosion. AE data along with half-cell potential measurements were recorded during the test to determine the stages and the overall deterioration process. Afterwards, the steel strands were removed from the specimens, cleaned and weighed; then the results were evaluated vis-à-vis Faraday's law with respect to the degree of corrosion present in each block.*

1. INTRODUCTION

Recent studies by the American Society of Civil Engineers (ASCE) show that more than 26% of the nation's bridges are either structurally deficient or functionally obsolete. While some progress has been made in recent years to reduce the number of deficient and obsolete bridges in rural areas, the number in urban areas is rising (Liu and Weyers, 1998). A $17 billion annual investment is needed to substantially improve current bridge conditions. Currently, only $10.5 billion is spent annually on the construction and maintenance of bridges (Almusallam, 2001). The ASCE Report Card provides a D average for America's overall infrastructure quality, where deteriorating conditions and inflation have added almost a trillion dollars to the total repair cost and maintenance since the last report card was published in 2005.

Bridge structures were presented with a C average under the ASCE guideline, proving that most of these constructions have been poorly maintained, and are unable to meet current and future demands, and in some cases, unsafe. It is crucial to keep in mind that a healthy transportation infrastructure is the backbone of a progressive economy. Therefore, a clear need exists towards developing effective non-destructive testing methods and proper evaluation criteria assessment of the damage level and residual life of bridge structures in the United States.

Corrosion of reinforcing steel is the most common source of deterioration in concrete bridges. Concrete protects the reinforcement by passivation. A resistant oxide forms surrounding the reinforcement, where a pH of 13-14 may be found adjacent to the steel. Corrosion of the steel reinforcement may occur at pH levels of 11 and lower. In seawater environments the pH may reach

a value of 8, creating the worst case scenario for corrosion (Austin et al., 2004).

The main problems with chloride induced corrosion is not only that the mechanical strength of the steel reinforcement is reduced, but also the corrosion product exerts stress into the concrete structure producing cracks that deteriorate the steel-concrete bond, which directly affects the serviceability performance. When a rebar starts to corrode, a gradual decrease of its diameter is produced, together with the generation of an oxide of higher volume than that of steel (Andrade et al., 1993). The unit volume of the final corrosion product $Fe(OH)_3 \cdot 3H_2O$ is as large as six and a half times of the original Fe volume (Li et al., 1998). Steel reinforcement bond is weakened due to the high porosity of the corrosive product around the steel, shown in Figure 1. In addition, corrosion decreases the cross sectional area of the steel strands minimizing their ductility and increasing stress concentrations at the reinforcement interface (Yoon et al., 2000).

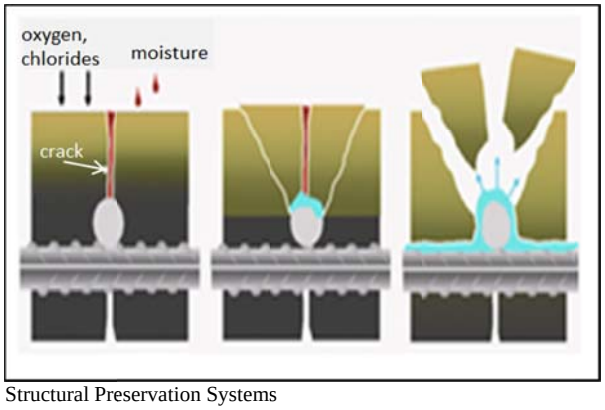

Structural Preservation Systems

Figure 1: Effect of corrosion product on concrete

This process affects prestressed structures durability the same way: (i) reduces the cross-section of the prestressed reinforcement, thereby, decreasing the load bearing capacity, and (ii) degrades the integrity of the surrounding concrete (Jaffer and Hansson, 2009). The longitudinal cracks created along the reinforcement after the expansive product is formed may affect the load bearing capacity of the components undergoing this distress, resulting in a decrease of service life of the structure.

Acoustic Emission (AE) sensing has been employed during the past 20 years as effective non-destructive technique for the detection, location, and monitoring of fatigue damages in metallic structures, as well as for concrete bridges (Li et al., 1998). This method has shown to be the most accurate and efficient; still, up to date it has not been fully exploited and studied. The damage detection sequence consists of remote sensors that detect elastic stress waves in the form of acoustic bursts, generated by a rapid release of energy from a localized source within a stressed material. Figure 2 illustrates a schematic of AE data acquisition.

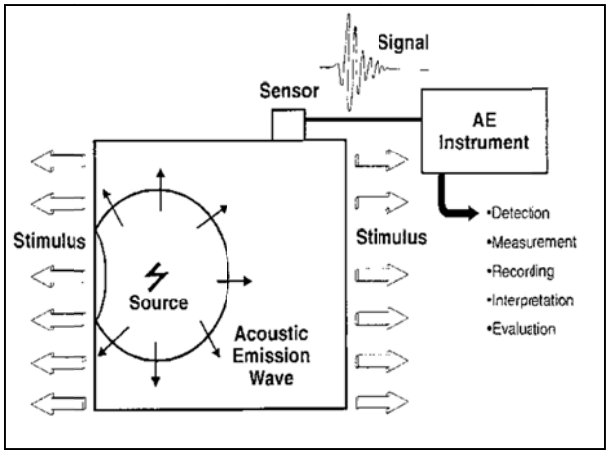

Mistras Group

Figure 2: Schematic of AE sensing process

Detection and analysis of AE signals may provide valuable information regarding the origin and importance of a discontinuity in a material. Because of the versatility of AE monitoring, this technique has many industrial applications and is used extensively as a research tool. AE monitoring of steel reinforced concrete has been shown to detect film cracking, gas evolution, and micro-cracking. It is also possible to use the AE method to calculate the location where the steel corrosion is occurring. This appears to be a promising technique that can be used as a method of quantifying the condition of steel reinforced concrete where corrosion is occurring. AE success on determining the onset of corrosion on steel reinforced concrete structures is due to its ability of detecting the acoustic energy emitted when an object is undergoing stress, such as when corrosion products form on the steel and push against the surrounding concrete (Seah et al., 1993). The primary advantage of AE sensing in comparison to other NDT methods is that it relies primarily on the process of flaw growth. The capability of detecting a weak stress wave makes it a strong candidate for the early detection and progression of reinforcement corrosion.

Furthermore, AE testing typically provides immediate information that may relate to the distress or risk of failure of a component.

2. RESEARCH SIGNIFICANCE

The Federal Highway Infrastructure estimates that 42 percent of the nearly 600,000 bridges in the Unites States are structurally deficient and in need of rapid repairs; this same percentage of bridges square footage fall in the 20 year-old category prime candidates for rehabilitation (Guthrie, et al.2002). Corrosion of

reinforcement steel is a main durability issue for concrete structures present in coastal areas and in countries where de-icing salts are routinely used (Inaudi, et al., 2009). The corrosion process has been represented as two transition periods where deterioration is the inverse of durability and a function of time. The two transition periods are defined as the onset of corrosion and the nucleation of cracking. The onset of corrosion separates the dormant stage from the initiation stage; the nucleation of cracking separates the initiation phase (II) from the accelerated phase (III). In Phase I the corrosion process is initiated, the rate of corrosion is controlled by the rate of transport oxygen. Eventually the flow of oxygen is inhibited and the corrosion loss decreases in Phase II. It is crucial to identify these transition periods to assess the durability of concrete structures because harmful cracks could occur in the concrete due to the expansion of corrosion product in Phase III (Ohtsu and Tomoda, 2008). Figure 3 shows the phases of corrosion.

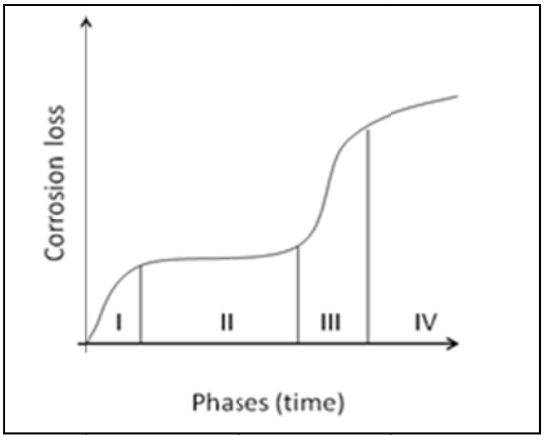

Figure 3: Corrosion phases

In bridge structure analysis, the AE device are essentially a piezoelectric crystal mounted to the surface of the beam, which detects mechanical shock waves and convert them into electrical signal that is amplified and processed by the sensors. The piezoelectric principle states that some materials produce a voltage when mechanically strained (direct effect). The inverse effect recognizes that these materials will deform if a voltage is applied to them.

Acoustic emission equipment is relatively simple to setup and sensors can be applied quickly. It is well suited to situations with limited accessibility because a single sensor can detect damage throughout a large portion of the structure. Multiple sensors can be used to locate the area of AE activity by triangulation or the activity of a single sensor can be used to provide an indication of the general area of damage (Ridge, and Ziehl, 2006).

3. EXPERIMENTAL WORK

The main purpose of the experiments is to analyze the validity of employing AE sensing to identify the corrosion process in steel reinforced concrete components.

Five concrete blocks with embedded prestressing steel strands were corroded using a controlled galvanic cell reaction and monitored with AE sensors and half-cell potential. Concrete blocks were either core drilled to reach the steel strand or pre-loaded to form surface cracks. Specimens were immersed in a 3.5% NaCl solution at room temperature. Two primary stages will be basis of AE activity identification: corrosion initiation (stage I), and corrosion propagation (stage II). Stage I will culminate after the chloride ions permeate the concrete cover and accumulate in the surroundings of the steel reinforcement, thereby breaking down the passive layer of the reinforcement. Stage II is intended as the process through which the rate of corrosion is accelerated and cracking and spalling of the concrete cover occur.

Half-cell potential and galvanic current measurements were taken to identify corrosion initiation, and then AE data were used to assess the corrosion propagation stage. Faraday's law represents the amount of steel mass consumed shown in equation (1).

$$\text{Mass loss (g)} = \frac{Mit}{zF} \qquad (1)$$

Where;

M: molecular weight (55.487 g/mol)
i: Current (A)
t: time (seconds)
z: Atomic number (2)
F: Faraday's constant (96,487)

The amount of corrosion is related to the electrical energy consumed, which is a function of voltage, amperage, and time interval (Auyeung, Balaguru and Chung, 2000). Corrosion of the prestressing strands will be defined as a percentage of the mass lost to the total mass of the strand. This formula states that:

- The mass of a substance formed or consumed in electrolysis is proportional to the amount of charge passing through it and to its molar charge;
- The mass of a substance formed or liberated is inversely proportional to the number of electrons per mole needed to cause the indicated change oxidation state.

The quantity of charge applied for any given electrolysis is given by the product of time (s) and current (A). For the corrosion process, for each mole of

iron oxidizes, 2 moles of electrons are lost, consuming a charge of 2 x 96,487 coulomb.

3.1 Test specimens and installation

Five concrete blocks with a 12 mm diameter steel strand embedded at the centerline of the blocks were cast to be examined and monitored under accelerated corrosion. The block measurements were 100 mm by 100 mm, with a length of 200 mm. The length of the steel strand was 300 mm so that the ends of the strand were exposed and connected to the electrical circuit. Two R6I AE sensors were installed on the surface of each specimen as shown in Figure 4. Half-cell potential measurements were recorded during the test in order to be related to the AE data.

Figure 4: Concrete blocks with AE sensors

In order to corrode the prestressing strands, specimens were immersed in a 3.5% NaCl solution which served as electrolyte for the galvanic cell reaction where a copper plate was connected to the positive (+) terminal of a DC Power Supply forming the cathode while the negative (-) terminal was connected to the steel reinforcement strand forming the anode. The specimens were drilled or pre-cracked so the saline solution could permeate the concrete and reach the steel prestressing strand and enable the galvanic cell reaction. Figure 5 shows a schematic of the accelerated corrosion setup, where the concrete block and copper plate were placed in a container in contact with the saline solution.

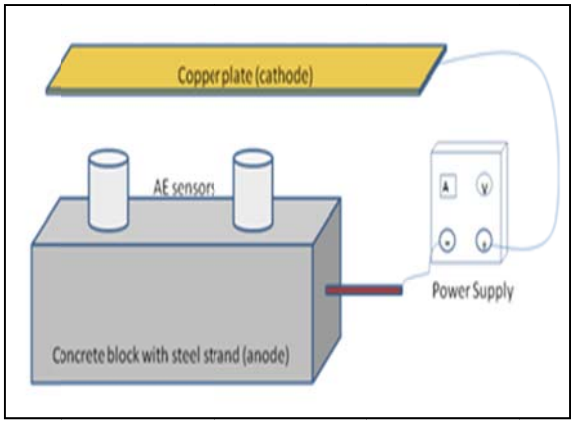

Figure 5: Accelerated corrosion test schematic

3.2 Equipment

Half-cell potential measurements were taken in accordance to ASTM C 876 using Elcometer 331 Covermeter and Copper-copper sulfate potential probe. ASTM C 876 states that if the measurement is more positive than -200 mV there is no corrosion; if it is more negative than -350 mV there is a greater than 90% probability of corrosion; and if it is between -200 mV and -350 mV there is uncertainty on the presence and degree of corrosion. Figure 6 shows how half-cell potential measurements were taken.

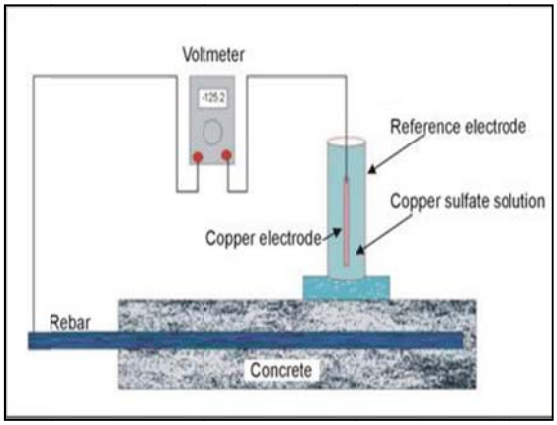

Federal Highway Administration

Figure 6: Half Cell Potential measurement setup

As mentioned, R6I acoustic emission sensors were used to monitor concrete blocks, these sensors were placed on each concrete block and continuously monitored using AE Win for DiSP software to investigate the sensors capability on detecting corrosion initiation and propagation. It was expected that two periods of high corrosion activity will be detected, the first to indicate the onset of corrosion, and the second one to indicate nucleation of crack due to the expansive corrosive products formed.

3.3 Test program

Five strands measuring 300 mm each were cut, weighed and embedded into the concrete. After preparing the concrete blocks, they were cured at room temperature and immersed into the electrolyte solution. A copper plate was placed in the container and along with the steel strand, connected to the power supply through the respective terminals. Figure7 shows a picture of the test setup.

Figure 7: Test setup for concrete block corrosion

Table 1: Test program

Test No.	Block No.	Current (A)	Time (s)
1	1	3.17	120,000
	2	3.00	120,000
2	3	0.10	582,000
		1.00	15,600
	4	0.10	582,000
		1.00	15,600
3	5	0.10	369,000
		0.84	256,800

The blocks were divided into three test groups as shown in Table 1. Blocks 1 and 2 were the first blocks to be examined; the exposed part of the strand inside the container was not protected against corrosion during this test. The current for block 1 was constant 3.17 A while for block 2 was 3 A. The test ran for approximately 33 hours and the strands were cleaned and their weights were measured at the end of the test. Blocks 3 and 4 were examined next; a current of 0.1 A was impressed during 162 hours, afterwards the current was raised to 1 A for only 4 hours to accelerate the corrosion activity. In this test, the exposed steel in contact with the electrolyte inside the container was covered with a corrosive resistant coating. It was noticed that the recorded voltage for block 4 is higher than 3; which is believed to be due to a discontinuity in the dipping of the strand facilitating the solution ingress in block 4. Block 5 was the last one to be tested, the current at the beginning of the test was 0.1 amps and continued for 102 hours, then the current was increased to 0.8 A for an additional 71 hours.

4. RESULTS AND DISCUSSION

The corrosion was monitored using two different techniques, half-cell potential and AE sensing. Half-cell potential measurements only provides an indication of whether there is corrosion activity in the concrete, therefore it was used to mark the onset of corrosion, but it does not have the ability to determine the rate of corrosion or its extent. The propagation stage was identified using the AE activity.

Faraday's law was used to theoretically determine the amount of mass loss of the prestressing strands, after each test the embedded strands were removed from the concrete, cleaned and weighed as specified by ASTM G-1. The measured weights were compared to the theoretical values from Equation 1.

4.1 Acoustic emission monitoring

The signal strength and the ability to source locate the area of activity are some of the AE parameters analyzed. Signal strength provides an indication of the corrosion initiation and propagation stages; source location determines whether the AE activity is occurring in the concrete-steel area and not recorded as outside noise. Test 1 has the shortest time duration due to the magnitude of the applied current. Half-cell potential measurements were recorded during the first hour for blocks 1 and 2 and shows detectable corrosion after 20 minutes and 40 minutes respectively. Signal strength graph for block 1 can be viewed in Figure 9; it indicates that corrosion was present in the specimen after 3 minutes of testing. The graph axes are signal strength (picoVolts-seconds, pVs) versus test time (seconds). Figure 10 is a representation of the source location technique; it may be observed that the corrosion activity (detected by energy released from the micro-cracks formed) is occurring between AE sensors mounted on the specimen.

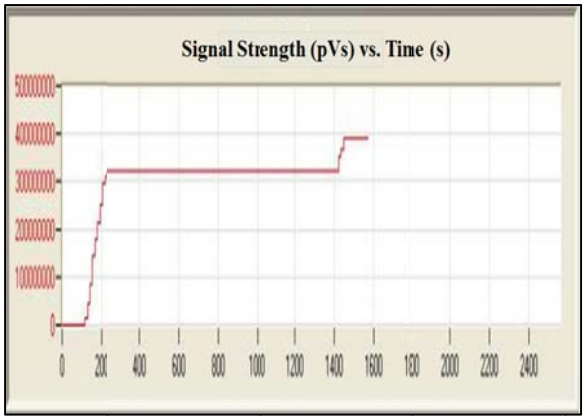

Figure 9: Signal Strength (pVs) vs. Time (s) for block 1 showing initiation of corrosion

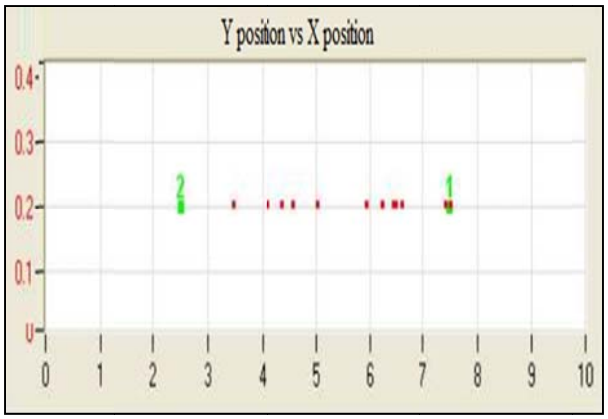

Figure 10: Source location for AE activity block 1

Figure 9 show that the initiation of corrosion started by a rapid increase in the cumulative signal strength due to the high current, forming the galvanic cell immediately after powering the system. The same results were achieved from block 2 but with a time lag and a smaller value of signal strength. These results from the first test showed the ability of AE sensing in detecting the corrosion faster than the half-cell potential measurements. Due to the exposure of the prestressing steel strand outside the concrete, these initial data show a relatively large AE activity at the beginning of the test which decreased later. The test setup was modified by coating the exposed parts of the prestressing strands with a corrosion resistant coating.

Test 2 was programmed to extend for a longer period of time while impressing a smaller current, making it possible to detect the different corrosion stages with ease. In the AE data obtained from this test, a visible difference was present in the results for blocks 3 and 4 due to a poor application of the plastic sealant. The corrosion in block 3 initiated after approximately 500 min and this was verified by the half-cell potential readings which gave a value of -550 mV, indicating corrosion activity. Signal strength at this time was 100,000 pVs. For block 4, the onset of corrosion occurred at approximately 42 minutes, when the signal strength value increased from $1.5x10^5$ to $3.5x10^5$ pVs. The second stage of the corrosion process was estimated to be after 9350 minutes for block 3, where the AE data shows a steep slope in signal strength. The ability of AE sensing to detect the rate of corrosion is illustrated in Figure 11 as when the current was raised from 0.1 to 1 A, an increase in the slope of signal strength vs. current occurred showing that the rate of corrosion was increased. The maximum cumulative signal strength is $1.1x10^6$ pVs.

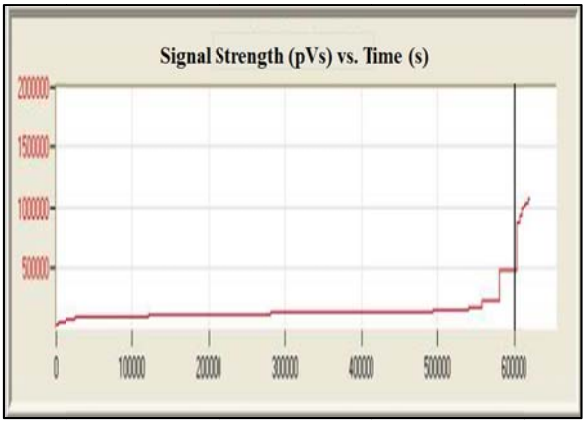

Figure 11: Signal Strength (pVs) vs. Time (s), block 3

For block 4, the propagation stage started after 1660 minutes. It is also clear from Figure 12 that AE data has the ability to detect the increase in the rate of corrosion when the current was raised. Yet linking this increase to the actual rate of corrosion is not achieved.

Figure 12: Signal Strength (pVs) vs. Time (s), block 4

Corrosion initiation for block 5 was determined to be at 650 minutes, at which the signal strength value was $1.5x10^5$ pVs, this was verified using half-cell potential measurements which were taken afterwards. The current was raised to 0.84 A after 6150 minutes and the point at which corrosion propagation is estimated to be starting was assumed to be after 8500 minutes where a jump is noticed in the cumulative signal strength graph, shown in Figure 13. The overall maximum achieved cumulative signal strength was approxamately $2.2x10^7$ pVs.

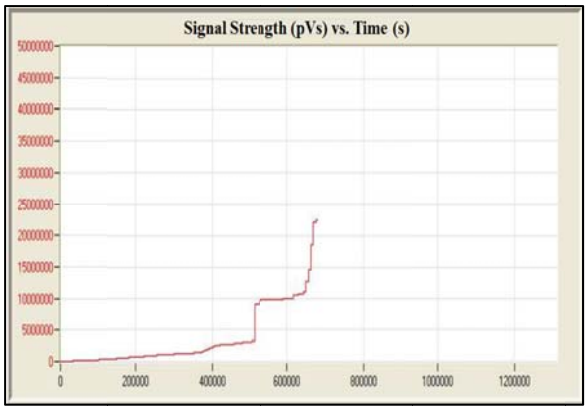

Figure 13: Signal Strength (pVs) vs. Time (s), block 5

The signal strength values presented in all tests are for two sensors. No certain value for signal strength can be chosen to define each stage of corrosion as the values were different for each test depending on the condition of concrete and the adequacy of the anti-corrosion coating used to cover the exposed parts of the prestressing strands used. Yet this technique needs to be generalized by employing different ranges of AE activity in terms of signal strength to differentiate between the different stages of corrosion. For this purpose, filtering of the AE data is crucial to differentiate between the corrosion activity, noise, and AE data captured form other types of energy released causing activities such as loading. Waveforms may provide a valuable means to filter the data due to their uniqueness regarding a certain activity (waveforms captured from corrosion activity are different from those captured from loading). Figure 14 shows one of the waveforms captured during the test. This generalized approach needs also to be related to the number of sensors used over a certain area, and the depth of the prestressing strands.

The source location technique provided by AE sensing shows that there is an activity taking place at the location of the strands. Overall, using cumulative signal strength to detect corrosion promises to be a good strategy to detect corrosion initiation and progression.

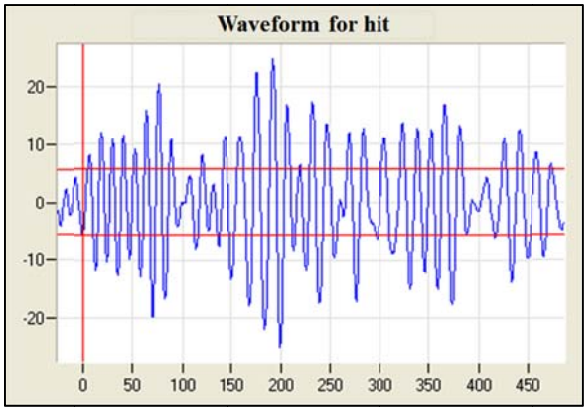

Figure 14: Waveform for a hit during corrosion activity

4.2 Steel mass loss results

Faraday's law was used to calculate the theoretical weight loss of the steel strands after corrosion. Each was carefully removed and weighed after each test. The results are reported in Table 2.

Table 2: Experimental and theoretical mass loss

Block No.	Original mass (g)	Theoretical mass loss (g)	Experimental mass loss (g)
1	221.0	109.4	111.8
2	232.6	103.5	108.8
3	231.2	21.2	31.5
4	232.6	21.2	32.0
5	232.7	69.7	78.7

Theoretical mass losses calculated with Faraday's law show some differences with respect to experimental mass losses. This is due to the fact that Faraday's law is employed to analyze mass loss of stand-alone steel, and the present experimental setup analyzes steel embedded in concrete.

5. CONCLUSIONS

Conclusions for the following test can be drawn as:

1. AE sensing is a promising NDT technique for detecting corrosion in steel reinforced concrete members because of its ability to detect corrosion activity.
2. Detecting the change in the rate of corrosion can be accomplished using AE data.
3. AE cumulative signal strength can detect the main stages of corrosion; initiation and propagation.

4. AE has the ability to detect the on-set of corrosion earlier than half-cell potential measurements which is one of the most common NDT methods used to detect corrosion.
5. The presence of corrosion activity can be verified from AE data represented in wave-forms, while the location where AE activity is generated can be determined using source location triangulation abilities.

For future work, a generalized approach should be developed to validate the use of AE sensing in a field environment and to link AE data with different stages of corrosion.

ACKNOWLEDGMENT

This work is performed under the support of the U.S. Department of Commerce, National Institute of Standards and Technology, Technology Innovation Program, Cooperative Agreement Number 70NANB9H9007. The authors wish to acknowledge those involved at Mistras Group (especially Didem Ozevin, Valery Godinez, and Richard Gostautas); University of South Carolina (Juan Caicedo); and joint venture partners University of Miami (Antonio Nanni and Brian Metrovich) and Virginia Tech (Dan Inman).

REFERENCES

(Almusallam, 2001) A. Almusallam. Effect of Degree of Corrosion on the Properties of Reinforcing Steel Bars, Construction and Building Materials, Volume 15, pp. 361-368, 2001.

ASTM C-876, (1991-Reapproved 1999), "Standard test method for half-cell potentials of uncoated reinforcing steel in concrete", American Standard for Testing and Materials, pp. 1-6.

ASTM G-1, (2003) "Standard Practice for Preparing, Cleaning, and Evaluating Corrosion Test Specimens", American Standard for Testing and Materials, pp. 1-9.

(Austin et al., 2004) S. Austin, R. Lyons, and M. Ing. Electrochemical Behavior of Steel-Reinforced Concrete During Accelerated Corrosion Testing, Corrosion, Volume 60, No. 2, pp. 203-212, 2004.

(Auyeung, Balaguru and Chung, 2000) Y. Auyeung, P. Balaguru, and L. Chung, Bond Behavior of Corroded Reinforcement Bars, ACI Materials Journal, Vol. 97, No. 2, pp. 212-220, 2000.

(Fricker and Vogel, 2007). S. Fricker and T. Vogel. Site Installation and Testing of Continuous Acoustic Monitoring, Construction and Building Materials, Volume 21, pp. 501-510, 2007.

(Guthrie, et al.2002). J. Guthrie, B. Battat, and C. Grethlein. Guthrie, Accelerated Corrosion Testing, The AMPTIAC Quarterly, Vol. 6, No. 3, pp. 11-14, 2002.

(Inaudi, et al., 2009) D. Inaudi, L. Manetti, B. Glisic, Reinforced Concrete Corrosion Wireless Monitoring System, 4th International Conference on Structural Health Monitoring on Intelligent Infrastructure (SHMII-4), pp. 2-7, 2009.

(Jaffer and Hansson, 2009). S. Jaffer and C. Hansson. Chloride-Induced Corrosion Products of Steel in Cracked-Concrete Subjected to Different Loading Conditions, Cement and Concrete Research, Volume 39, pp. 116-125, 2009.

(Li, et al., 1998). Z. Li, A. Zdunek, E. Landis, and S. Shah. Application of Acoustic emission Technique to Detection of Reinforcing Steel Corrosion in Concrete, ACI Materials Journal, Vol. 95, No. 1, pp. 68-76, 1998.

(Liu and Weyers, 1998) Y. Liu and R. Weyers. Modeling the Time-to-Corrosion Cracking in Chloride Contaminated Reinforced Concrete Structures, ACI Materials Journal, No. 95-M65, pp 675-680, 1998.

(Ohtsu, M., and Tomoda, Y., 2008), M. Ohtsu, and Y. Tomoda. Phenomenological Model of Corrosion Process in Reinforced Concrete Identified by Acoustic Emission, ACI Materials Journal, Vol. 105, No. 2, pp. 194-199, 2008.

(Ridge, and Ziehl, 2006) A. Ridge and P. Ziehl. Evaluation of Strengthened Reinforced Concrete Beams:Cyclic Load Test and Acoustic Emission Methods, *ACI Structural Journal*, Technical paper 103-S84, pp. 832-841, 2006.

(Seah, et al., 1993) K. Seah, K. Lim,S. Chew, and S. Teoh. The Correlation of Acoustic Emission with Rate of Corrosion, *Corrosion Science*, Vol. 34, No. 10, pp. 1707-1713, 1993.

(Yoon, et al., 2000) D. Yoon, W. Weiss and S. Shah. Assessing Damage in Corroded Reinforced *Concrete* Using *Acoustic* Emission, *Journal of Engineering Mechanics*, Vol. 126, No. 3, pp. 273-283, 2000.